Rovibrational internal energy excitation and dissociation of nitrogen in hypersonic flows

By   M. Panesi†, T. E. Magin‡, A. Munafó‡, A. Bourdon¶, R. Jaffe
AND D. W. Schwenke

A rovibrational collisional model is developed to study the internal energy excitation and dissociation processes behind a strong shockwave in a nitrogen flow. The reaction rate coefficients are obtained from the *ab initio* database of NASA Ames Research Center. The master equation is coupled with a one-dimensional flow solver. The system of equations is solved for conditions expected for reentry into Earth's atmosphere at 10 km/s. In addition, a coarse graining model is proposed by lumping the rovibrational energy levels into a smaller number of bins. The results obtained by means of the full rovibrational collisional model are compared to those obtained by means of a vibrational collisional model. Thermalization and dissociation occurs after a larger distance for the rovibrational collisional model compared to the distance predicted by means of the vibrational collisional model. This is expected to be the consequence of the assumption of equilibrium between the rotational energy and the translational energy, used for the vibrational collisional model, as opposed to the rovibrational collisional model. Finally, the coarse graining model allows an accurate description of the internal energy relaxation and dissociation processes based on a reduced number of equations.

1. Introduction

Prediction of the radiative heat flux to the surface of a spacecraft entering a planetary atmosphere strongly depends on the completeness and accuracy of the physical model used to describe the nonequilibrium phenomena in the flow. During an atmospheric entry, the translational energy of the fluid particles drastically rises through a shock. Depending on the intensity of the shock, different physico-chemical processes may take place, such as excitation of the internal energy modes, dissociation of the molecules, ionization of the atoms and molecules. These nonequilibrium phenomena are strongly coupled to each other. For re-entry velocities >10 km/s, a significant portion of the heating experienced by the heat shield can be due to radiation and is highly influenced by the shape of the internal energy distribution function. Understanding thermo-chemical nonequilibrium effects is also important for a correct interpretation of experimental measurements in flight and in ground wind-tunnels. Concentration of the gas species and distribution of their internal energy level populations can be estimated by means of either multi-temperature models (Park 1990) or collisional radiative models (Panesi *et al*. 2009). Collisional radiative models take into account all relevant collisional and radiative mechanisms between the internal energy levels of the different species in the flow. They constitute a valid alternative to the multi-temperature models since they exhibit a wider range of applicability.

This work is at the interface between computational chemistry and computational fluid

† Institute for Computational Engineering and Sciences, The University of Texas at Austin
‡ Aeronautics and Aerospace Department, von Karman Institute for Fluid Dynamics, Belgium
¶ EM2C, CNRS UPR 288 – Ecole Centrale Paris, France

dynamics and aims at developing new models based on microscopic theory and applying them to macroscopic scale. We have recently used the database developed at NASA Ames Research Center to derive a 1D Vibrational Collisional (VC) model and to simulate a shock in a nitrogen flow (Bourdon *et al.* 2008; Magin *et al.* 2009). This model, so far only collisional, is the first component of a larger model for air that will eventually include radiation. In the present work, we propose to relax the assumption of Maxwell-Boltzmann distribution for the rotational energy levels by developing a RoVibrational Collisional (RVC) model coupled with a flow solver. First, the full master equation is used. Then, the energy levels are lumped into bins as a function of their global internal energy, independently of their vibrational and rotational contributions, based on a uniform distribution of the levels within a bin. Both collisional models are used for the simulation of a shock in a nitrogen flow. The collisional conditions are carefully selected to stay in the validity range of a simplified mechanism for the $N_2 + N$ system comprising dissociation and VT relaxation. We study the convergence of the number of bins for the bin populations, using the solution based on the full master equation as a reference. Finally, we compare the results obtained by means of the rovibrational collisional model to the previously developed VC model.

2. NASA Ames database

The NASA Ames database (Schwenke 2008; Jaffe *et al.* 2009, 2010) comprises 9390 (v, J) rovibrational levels for the electronic ground-state of nitrogen, where index v stands for the vibrational quantum number, and index J, the rotational quantum number. These levels can also be denoted by means of a global index i, sorting them, in this work, by increasing value of energy. The relation between the i and (v, J) notations is expressed as

$$i = i(v, J), \quad v = 0, \ldots, v_{\max}, \quad J = 0, \ldots, J_{\max}(v).$$

Conversely, the relation between the (v, J) and i notations is given by the relations

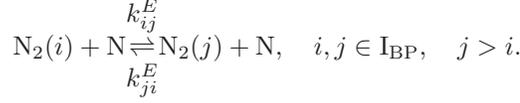$$v = v(i), \quad J = J(i), \quad i \in \mathrm{I_{BP}},$$

where $\mathrm{I_{BP}}$ is the set of global indices for the nitrogen energy levels. Most of these levels are truly bound, *i.e.*, their energy is lower than the dissociation energy relative to the level $(v = 0, J = 0)$, equal to 9.75 eV for the electronic ground-state of nitrogen, while some of the energy levels are predissociated, *i.e.*, their energy is higher than the dissociation energy relative to the level $(v = 0, J = 0)$. The bound energy levels are denoted by the set $\mathrm{I_B}$, and the predissociated energy levels by the set $\mathrm{I_P}$. The set for all the levels is then given by $\mathrm{I_{BP}} = \mathrm{I_B} \cup \mathrm{I_P}$. The database for the $N_2 + N$ system comprises more than 23 million reactions, for dissociation of truly bound states and predissociated states,

$$N_2(i) + N \underset{k_i^{Db}}{\overset{k_i^{Df}}{\rightleftharpoons}} N + N + N, \quad i \in \mathrm{I_{BP}},$$
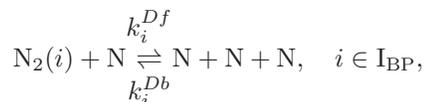
for predissociation of the predissociated states,

$$N_2(i) \underset{k_i^{Pb}}{\overset{k_i^{Pf}}{\rightleftharpoons}} N + N, \quad i \in \mathrm{I_P},$$
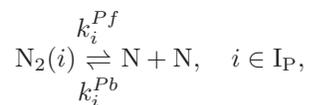
and for excitation between all states

$$N_2(i) + N \underset{k_{ji}^E}{\overset{k_{ij}^E}{\rightleftharpoons}} N_2(j) + N, \quad i,j \in I_{BP}, \quad j > i.$$

The direct reaction rate coefficients k_i^{Df}, k_i^{Pf}, and k_{ij}^E, $j > i$, are obtained based on the reaction cross-sections for nine values of the gas translational temperature (T=7500; 10,000; 12,500; 15,000; 20,000; 25,000; 30,000; 40,000; and 50,000 K). The reverse reaction rate coefficients k_i^{Db}, k_i^{Pb}, and k_{ij}^E, $j < i$, are computed based on microreversibility, using only endothermic rate coefficients, although some exothermic rates were also available

$$k_i^{Db}(T) = k_i^{Df}(T) \frac{g_i Q_{N_2}^t(T) \exp(\frac{-(E_i - 2E_N)}{k_B T})}{[g_N Q_N^t(T)]^2}, \quad i \in I_{BP}, \tag{2.1}$$

$$k_i^{Pb}(T) = k_i^{Pf}(T) \frac{g_i Q_{N_2}^t(T) \exp(\frac{-(E_i - 2E_N)}{k_B T})}{[g_N Q_N^t(T)]^2}, \quad i \in I_P, \quad j > i, \tag{2.2}$$

$$k_{ji}^E(T) = k_{ij}^E(T) \frac{g_i \exp(\frac{-(E_i - E_j)}{k_B T})}{g_j}, \quad i,j \in I_{BP}, \quad j > i, \tag{2.3}$$

where quantity E_i stands for the energy of level i and g_i, its degeneracy. The translational partition functions are defined as

$$Q_{N_2}^t(T) = \left(\frac{2\pi k_B m_{N_2} T}{h_P^2}\right)^{3/2}, \quad Q_N^t(T) = \left(\frac{2\pi k_B m_N T}{h_P^2}\right)^{3/2}, \tag{2.4}$$

where symbol k_B stands for Boltzmann's constant, and h_P, Planck's constant. The nitrogen atom degeneracy is $g_N = 12$ (nuclear and electronic spin contributions).

3. Rovibrational collisional models

Assuming that the flow is steady, the momentum conservation equations reads

$$\frac{d}{dx}(\dot{m}u + p) = 0, \tag{3.1}$$

where quantity $\dot{m} = \rho u$ stands for the mass flux; ρ, the mixture mass density; u, the flow velocity; and p, the mixture pressure. The mass density is computed based on the relation $\rho = n_{N_2} m_{N_2} + n_N m_N$, where quantity n_{N_2} is the molecular nitrogen number density, and n_N, the atomic nitrogen number density. The global enthalpy conservation equation is given by

$$\frac{d}{dx}(\dot{m}H) = 0, \tag{3.2}$$

where the total enthalpy is denoted by $H = \frac{1}{2}u^2 + E^t + p/\rho + E^{int}$, with the internal energy, E^{int}, and the translational energy $E^t = \frac{3}{2}(n_{N_2} + n_N)k_B T/\rho$. The mixture pressure is computed by means of the relation $p = \frac{2}{3}\rho E^t$, and the internal energy, by means of the expression $\rho E^{int} = m_{N_2} n_{N_2} E_{N_2}^{int} + m_N n_N E_N$. Two different RVC models are presented in this section. First, the full master equation for the energy levels $i \in I_{BP}$ is coupled with a flow solver. Then, an alternative approach is lumping the energy levels into bins as a function of their global internal energy, independently of their vibrational and rotational contributions. Let us define the set of indices for the energy levels of bin k as follows:

$$I_k = \{i \in I_{BP} \text{ such that } (\mathcal{E}_k \leq E_i < \mathcal{E}_{k+1})\}, \quad k \in K_{BP},$$

where K_{BP} is the set of indices for the bins. Quantities $\mathcal{E}_k$ allow for the energy grid to be defined either by using an energy grid or by lumping an arbitrary number of levels in a bin. The set K_B stands for the bins corresponding to bound energy levels, and the set K_P, for the bins corresponding to predissociated energy levels, with $K_{BP} = K_B \cup K_P$. It is important to avoid mixing bound and predissociated energy levels in the bin comprising the dissociation energy, because both types of levels show a distinct dynamical behavior.

3.1. *Full master equation*

The species continuity equations for the nitrogen atom and the rovibrational energy levels of molecular nitrogen are given by

$$\frac{d}{dx}(n_N u) = \omega_N, \tag{3.3}$$

$$\frac{d}{dx}(n_i u) = \omega_i, \quad i \in I_{BP}. \tag{3.4}$$

Defining the molecular nitrogen number density, $n_{N_2} = \sum_{i \in I_{BP}} n_i$, the molecular nitrogen internal energy is given by the expression

$$n_{N_2} E_{N_2}^{int} = \sum_{i \in I_{BP}} n_i E_i, \tag{3.5}$$

without any a priori assumption on the population. The initial population is assumed to follow a Maxwell-Boltzmann distribution

$$\frac{n_i}{n_{N_2}} = \frac{g_i}{Q(T, T_{int})} \exp\left(\frac{-E_i}{k_B T_{int}}\right), \quad i \in I_{BP},$$

at the internal temperature T_{int} equal to the freestream translational temperature. The total internal partition function is defined as $Q(T_{int}) = \sum_{j \in I_{BP}} g_j \exp[-E_j/(k_B T_{int})]$.

3.2. *Uniform distribution for the energy level populations in a bin*

The energy E_i for level i is constant in bin k and equal to the average energy

$$\bar{E}_k = \frac{\sum_{i \in I_k} g_i E_i}{\bar{g}_k},$$

based on the degeneracy of the levels. The energy level populations are assumed to be uniform within the bin $k \in K_{BP}$

$$\frac{n_i}{\bar{n}_k} = \frac{1}{\bar{g}_k} g_i, \quad i \in I_k, \tag{3.6}$$

with the degeneracy and number density for the bin

$$\bar{g}_k = \sum_{i \in I_k} g_i, \tag{3.7}$$

$$\bar{n}_k = \sum_{i \in I_k} n_i. \tag{3.8}$$

The species continuity equations for the nitrogen atom and the rovibrational energy levels of molecular nitrogen are obtained by means of Eq. (3.3) for atoms and Eq. (3.4)

	1	2	3
T [K]	300	62,546	11,351
p [Pa]	13	10,792	13,363
u [km/s]	10	2.51	0.72
$x_{\rm N}$ [−]	0.028	0.028	1

TABLE 1. Translational temperature, pressure, velocity, and nitrogen atom mole fraction for a $\rm N - N_2$ mixture in the ground electronic state: (1) chemical nonequilibrium thermal equilibrium collisional conditions; (2) post-shock nonequilibrium conditions at the shock location; (3) local thermodynamic equilibrium post-shock conditions.

for molecules summed over the energy levels of bin k

$$\frac{\mathrm{d}}{\mathrm{d}x}(n_N u) = \bar{\omega}_{\rm N}, \tag{3.9}$$

$$\frac{\mathrm{d}}{\mathrm{d}x}(\bar{n}_k u) = \bar{\omega}_k, \quad k \in \mathrm{K_{BP}}, \tag{3.10}$$

where the expressions for the chemical production rates for the nitrogen atom and the average rovibrational energy levels of molecular nitrogen can be found in Magin *et al.* (2010). The molecular nitrogen internal energy is given by the expression

$$n_{\rm N_2} E_{\rm N_2}^{int} = \sum_{k \in \mathrm{K_{BP}}} \bar{n}_k \bar{E}_k,$$

with the molecular nitrogen number density, $n_{\rm N_2} = \sum_{k \in \mathrm{K_{BP}}} \bar{n}_k$. The initial population of the bins is assumed to follow a Maxwell-Boltzmann distribution

$$\frac{\bar{n}_k}{n_{\rm N_2}} = \frac{\bar{g}_k}{\bar{Q}(T_{int})} \exp\left(\frac{-\bar{E}_k}{k_{\rm B} T_{int}}\right), \quad k \in \mathrm{K_{BP}},$$

at the internal temperature T_{int} equal to the freestream translational temperature. The total internal partition function is defined as $\bar{Q}(T_{int}) = \sum_{l \in \mathrm{K_{BP}}} \exp[-\bar{E}_l/(k_{\rm B} T_{int})]\bar{g}_l$. It is important to mention that the assumption of a uniform distribution of the energy levels in a bin does not allow for the system to reach equilibrium, in particular for a low number of bins, since the global population of energy levels cannot be formally expressed as a Maxwell-Boltzmann distribution.

4. Results

The $\rm N_2, N$ collisional gas mixture is assumed to be in chemical nonequilibrium and thermal equilibrium at p=13 Pa pressure and T=300 K translational temperature. A chemical nonequilibrium value of 2.8% mole fraction of N atoms was chosen to have enough nitrogen atoms in the flow, since only the mechanism for the $\rm N + N_2$ system is considered in this work. The collisional and post-shock conditions based on the jump relations are reviewed in Table 1, together with the post-shock Local Thermodynamic Equilibrium (LTE) conditions. The post-shock temperatures are calculated by freezing the internal (rotational and vibrational) energy for both the RVC and VC models. For all cases, the Rankine-Hugoniot relations yield conservation of the total enthalpy through the shock. Table 2 gives the Lagrangian time for a fluid particle and the corresponding distance from the shock for the full RVC model.

Lagrangian time [s]	Distance from the shock [m]	Lagrangian time [s]	Distance from the shock [m]
0	0	10^{-7}	2.5×10^{-4}
10^{-13}	2.5×10^{-10}	10^{-6}	2.5×10^{-3}
10^{-12}	2.5×10^{-9}	10^{-5}	2.5×10^{-2}
10^{-11}	2.5×10^{-8}	10^{-4}	2.5×10^{-1}
10^{-10}	2.5×10^{-7}	10^{-3}	1.3
10^{-9}	2.5×10^{-6}	10^{-2}	8.2
10^{-8}	2.5×10^{-5}		

TABLE 2. Lagrangian time for a fluid particle and corresponding distance from the shock for the full RVC model.
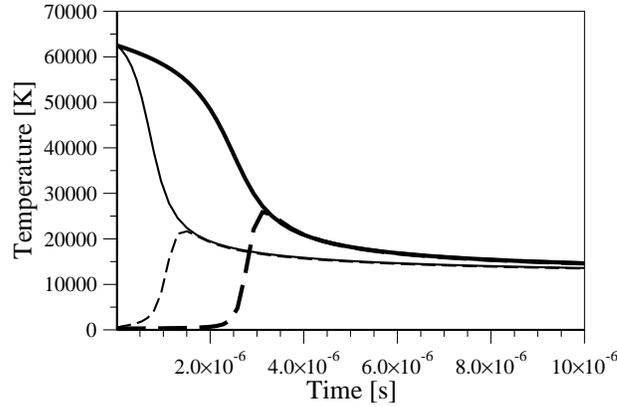

FIGURE 1. Post-shock translational temperature (unbroken line) and internal / vibrational temperature (dashed line) for a fluid particle as a function of the Lagrangian time starting at t=0 s with the shock, based on the collisional LTE conditions given in Table 1. Full RVC model (thick lines) and VC model (thin lines).

Figure 1 shows the translational temperature and the internal/vibrational temperature as a function of time for the RVC and VC models. For the full RVC model, an internal temperature is introduced based on the relative population among the rovibrational energy level $E(0, 10)$ and the ground level $E(0, 0)$:

$$T_{int} = \frac{E(0, 10) - E(0, 0)}{k_B \ln \left(\frac{n(0,10)}{n(0,0)} \right)}. \tag{4.1}$$

For the VC model, the vibrational temperature is defined based on the relative population among the first excited vibrational energy level $\tilde{E}_1$ and the ground level $\tilde{E}_0$, as follows:

$$T_v = \frac{\tilde{E}_1 - \tilde{E}_0}{k_B \ln \left(\frac{\tilde{n}_1}{\tilde{n}_0} \right)}, \tag{4.2}$$

where symbol $\tilde{n}_1$ stands for the population of the first excited level, and $\tilde{n}_0$, the population of the ground level. These definitions are justified considering that the thermodynamic state of the gas is mostly characterized by the population of the lowest energy levels, *i.e.*, highly populated. Thermalization is monotonic and occurs after a larger distance
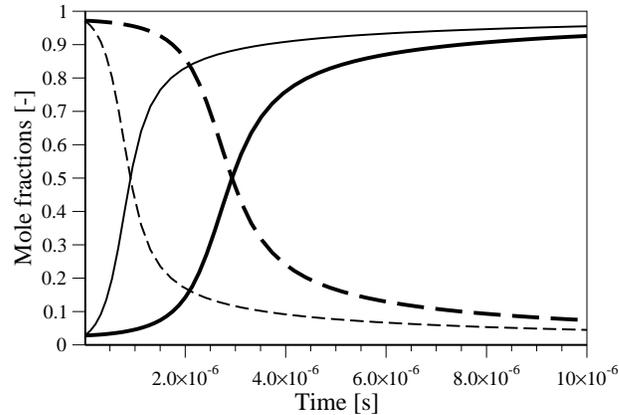
FIGURE 2. Post-shock nitrogen atom mole fraction (dashed line) and nitrogen molecule mole fraction (unbroken line) for a fluid particle as a function of the Lagrangian time starting at t=0 s with the shock, based on the collisional LTE conditions given in Table 1. Full RVC model (thick lines) and VC model (thin lines).
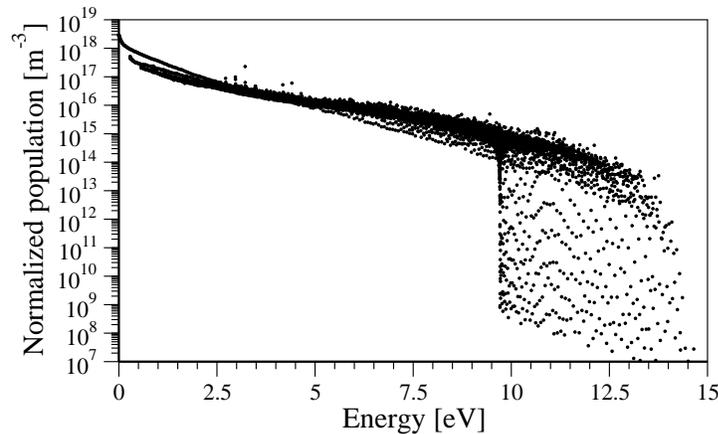

FIGURE 3. Post-shock population of the rovibrational energy levels for the nitrogen molecule as a function of their rovibrational energy at a Lagrangian time for a fluid particle $t = 2.6 \times 10^{-6}$ s, obtained by means of the full RVC model based on the collisional LTE conditions given in Table 1.

for the RVC model. The analysis of the mixture composition in Figure 2 shows that the RVC model has a longer incubation time than the VC model and a more gradual slope in the mole fractions after dissociation gets going. These imply a faster dissociation rate for the VC model. Both models reach the same equilibrium composition. Let us examine the post-shock populations of the rovibrational energy levels for the nitrogen molecule as a function of their rovibrational energy, at a Lagrangian time for a fluid particle $t = 2.6 \times 10^{-6}$ s (at a distance of $\sim 7 \times 10^{-3}$m from the shock), corresponding to the time for thermalization in Figure 1 and to the induction time for dissociation in Figure 2. At $t = 2.6 \times 10^{-6}$ s, the rovibrational populations exhibit a strong non-Boltzmann behavior, as shown in Figure 3. The rovibrational level populations are organized following distinct curves, clearly visible for the low energy levels. This phenomenon can be explained by tagging the energy levels with a common vibrational quantum number by means of
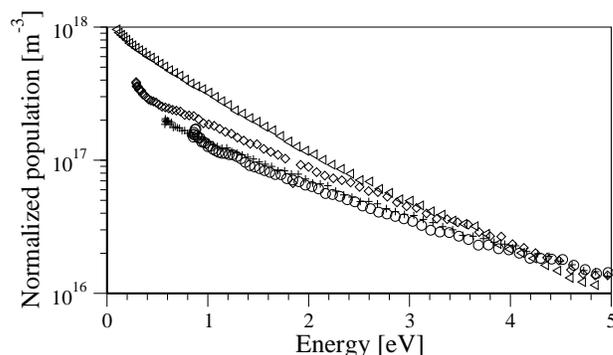
Panesi et al.

FIGURE 4. Close-up on the post-shock populations of the first four vibrational energy levels for the nitrogen molecule ($\triangleleft$ $v = 0$, $\diamond$ $v = 1$, $+$ $v = 2$, and $\circ$ $v = 3$), with their respective rotational temperature: $T_r(0) = 11\ 959$ K, $T_r(1) = 16\ 674$ K, $T_r(2) = 18\ 949$ K, and $T_r(3) = 20\ 098$ K, as a function of their rovibrational energy at a Lagrangian time for a fluid particle $t = 2.6 \times 10^{-6}$ s, obtained by means of the full RVC model based on the collisional LTE conditions given in Table 1.

distinct symbols. Figure 4 shows that these curves correspond to clusters of levels sharing the same vibrational quantum number. Therefore, we propose to extract, from the $n(v, J)$ population computed by using the full RVC model, a rotational temperature $T_r(v)$ for each vibrational energy level v. It is defined as follows:

$$\frac{\sum_{J=0}^{J_{max}(v)} n(v, J)\Delta E(v, J)}{\sum_{J=0}^{J_{max}(v)} n(v, J)} = \frac{\sum_{J=0}^{J_{max}(v)} g_J \Delta E(v, J) \exp\left(\frac{-\Delta E(v,J)}{kT_r(v)}\right)}{\sum_{J=0}^{J_{max}(v)} g_J \exp\left(\frac{-\Delta E(v,J)}{kT_r(v)}\right)}, \qquad (4.3)$$

where the rotational contribution to the energy of a rovibrational level is given by the expression $\Delta E(v, J) = E(v, J) - E(v, 0)$. The rotational temperatures $T_r(v)$ are computed by solving Eq. (4.3) by means of a Newton method; they are found to be increasing with the value of the vibrational quantum number. This leads us to question the widely used assumption of equilibrium between the translational temperature and the rotational temperature $T = T_r$ in compressed flows. This assumption could explain why thermalization and dissociation occurs after a larger distance for the full RVC model, compared to the distance predicted by both the multi-temperature model and VC model relying on the assumption that $T = T_r(v)$ for all v. Finally, we notice in Figure 3 that the population of some of the quasi-bound energy levels (levels above the dissociation energy of ~ 9.75eV) can be strongly depleted; this depletion is attributed to the predissociation reaction.

The coarse graining model based on a uniform distribution of the levels within a bin is applied to reduce the complexity of the full RVC model. Figure 5 shows the translational temperature as a function of time for the full RVC model and the bin model for different total number of bins. A poor convergence of the total number of bins is found when the predissociation reaction is considered. A specific treatment is being investigated for the predissociation reaction.

5. Conclusions

In this work, we have developed a 1D rovibrational collisional model to describe the internal energy relaxation and dissociation processes behind a strong shockwave in a nitrogen flow. The 9390 rovibrational energy levels of the nitrogen molecule of the *ab*
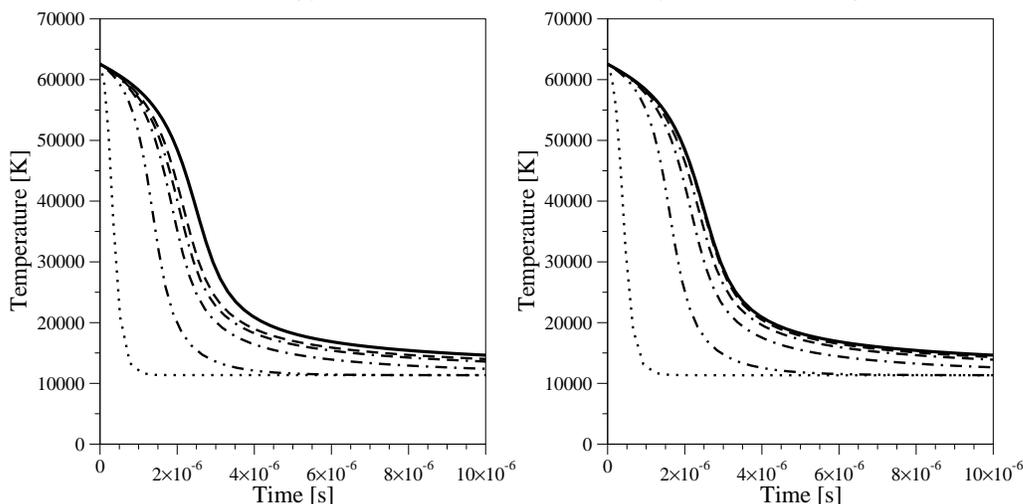
FIGURE 5. Post-shock translational temperature computed by means of the coarse graining RVC model with a uniform distribution of the energy levels within a bin ($\cdots$ 2, $-\cdot\cdot-$ 5, $\cdot-\cdot$ 10, $\cdot-\cdot-$ 20, $---$ 40 bins) and by means of the full RVC model (unbroken line), for a fluid particle as a function of the Lagrangian time, based on the collisional LTE conditions given in Table 1. Left: accounting for predissociation reactions in the chemical mechanism; right: not accounting for predissociation reactions.

initio NASA Ames database are taken into account in the master equation for mass conservation, coupled with conservation equations for momentum and total energy. A coarse graining model has been proposed by lumping the $N_2(v, J)$ energy levels into a smaller number of bins based on a uniform distribution of the levels within a bin. The results obtained by means of the full RVC model have been compared to those obtained by means of a vibrational collisional model (Bourdon *et al.* 2008; Magin *et al.* 2009). We have clearly shown that thermalization occurs after a larger distance for the full RVC model compared to the distance predicted by the VC model. Dissociation is also delayed when predicted by the full RVC model. This is ex pected to be the consequence of the assumption of equilibrium between the rotational energy and the translational energy used for the VC model, as opposed to the full RVC model. The uniform distribution bin model allow us to describe accurately the internal energy relaxation and dissociation processes based on a reduced number of equations. Lessons learned from studying the $N_2(v, J) + N$ system by means of the uniform-distribution bin model will allow the $N_2(v, J) + N_2(v', J')$ system presented by Jaffe *et al.* (2010) to be investigated. Indeed, it is no longer possible to compute and tabulate rate coefficients for all possible combinations of initial (v, J) and (v', J') levels of the colliding N_2 molecules.

A second type of coarse graining model can be based on a Maxwell-Boltzmann distribution of the levels within a bin. This model allows the system to reach equilibrium at the fine-grain level since the global population of rovibrational energy can be formally expressed as a Maxwell-Boltzmann distribution, as opposed to the uniform-distribution bin model. This property is expected to play an important role in developing a reduced model suitable for computational fluid dynamics applications, where the number of bins will be kept low. Another type of collisional model is currently being developed by Liu *et al.* (2010) based on a multi-group maximum entropy principle with the macroscopic

parameters as constraints. The equations for the macroscopic parameters, including the macroscopic rate coefficients, are obtained from moments of the master equations.

Acknowledgements

REFERENCES

BOURDON, A., PANESI, M., BRANDIS, A., MAGIN, T. E., CHABAN, G., HUO, W., JAFFE, R. & SCHWENKE D. W. 2008 Simulation of flows in shock-tube facilities by means of a detailed chemical mechanism for nitrogen excitation and dissociation. *Proceedings of the Summer Program 2008*, Center for Turbulence Research, Stanford University, NASA Ames Research Center.

JAFFE, R., SCHWENKE, D. & CHABAN G. 2009 Theoretical analysis of N_2 collisional dissociation and rotation-vibration energy transfer. *AIAA 2009-1569, 47th AIAA Aerospace Sciences Meeting and Exhibit*, Orlando, Florida.

JAFFE, R., SCHWENKE, D. & CHABAN, G. 2010 Vibration-rotation excitation and dissociation in $N_2 - N_2$ collisions from accurate theoretical calculations. *AIAA-2010-4517, 10th AIAA/ASME Joint Thermophysics and Heat Transfer Conference*, Chicago, Illinois.

LIU, Y., VINOKUR, M., PANESI, M. & MAGIN, T. 2010 Multi-group maximum entropy model for thermo-chemical nonequilibrium. *AIAA-2010-4332, 10th AIAA/ASME Joint Thermophysics and Heat Transfer Conference*, Chicago, Illinois.

MAGIN, T. E., PANESI, M., BOURDON, A., W., JAFFE, R. & SCHWENKE D. W. 2009 Internal energy excitation and dissociation of molecular nitrogen in a compressing flow. *Proceedings of the Summer Program 2008, AIAA 2009-3837, 41st AIAA Thermophysics Conference*, San Antonio, Texas.

MAGIN, T. E., PANESI, M., BOURDON, A., W., JAFFE, R. & SCHWENKE D. W. 2010 Rovibrational internal energy excitation and dissociation of molecular nitrogen in hypersonic flows. *AIAA-2010-4336, 10th AIAA/ASME Joint Thermophysics and Heat Transfer Conference*, Chicago, Illinois.

PANESI, M., MAGIN, T., BOURDON, A., BULTEL, A., CHAZOT, O. 2009 Analysis of the Fire II flight experiment by means of a collisional radiative model. *Journal of Thermophysics and Heat Transfer*, **23** 236.

PARK, C. 1990 *Nonequilibrium hypersonic aerothermodynamics*. Wiley, New York.

SCHWENKE, D. 2008 Dissociation cross-sections and rates for nitrogen. *VKI LS 2008, Non-equilibrium Gas Dynamics, from Physical Models to Hypersonic Flights*, Rhode-Saint-Genèse, Belgium.